

Design of a Compact Planar UWB MIMO Antenna with Enhanced Isolation for Diversity Applications

Ningappa T Pujar¹, Dr. S Jagadeesha², Dr. Prathibha Kiran³, Dr. Sharath Kumar A J⁴

¹ Assistant Professor, Dept of Computer Science & Engineering, Tontadarya College of Engineering, Gadag, Karnataka, India. ningappap@gmail.com

² Professor, Department of Electronics and Communication Engineering, AMC Engineering College, Bengaluru, Karnataka, India. jagadeesh.sd69@gmail.com

³ Associate professor, Department of Electronics and Communication Engineering, AMC Engineering College, Bengaluru, Karnataka, India. prathibha.kiran@amceducation.in

⁴ Associate Professor, Department of Electronics and Communication Engineering, Vidyavardhaka College of Engineering, Mysuru, Karnataka, India. sharathkumar.aj@vvce.ac.in

^{1,2,3,4} Affiliated to Visvesvaraya Technological University, Belagavi, Karnataka, India

ARTICLE INFO

ABSTRACT

Received: 17 Dec 2024

Revised: 21 Feb 2025

Accepted: 28 Feb 2025

This paper presents the design and simulation of a 2×2 Koch fractal antenna array with metamaterial in HFSS for UWB applications. The antenna operates from 3 GHz to 13 GHz with a return loss below -10 dB and resonance at 3.8 GHz and 12 GHz. Mutual coupling is reduced below -40 dB (simulated) and -50 dB (measured). The radiation patterns show close agreement, with a maximum variation of 0.05–0.1 dB. The multiplexing efficiency exceeds 60%, and the ECC remains below 0.02, confirming excellent isolation and diversity, making it suitable for high performance UWB systems.

Keywords: Fractal Antenna, Metamaterial, Mutual Coupling, Ultra-Wideband (UWB)

INTRODUCTION

In today's rapidly advancing technological landscape, wireless communication systems must become more accessible, faster, and more reliable. Ultra-wideband (UWB) is one of the promising technologies, having high data rate, great bandwidth, and minimum power density. The UWB frequency range 3.1 GHz to 10.6 GHz, a bandwidth of 7.5 GHz.

A new technique has been presented in [1], suggesting a small four-element multiple-input multiple-output (MIMO) antenna with greatly minimized mutual coupling throughout the whole UWB band. This technique combines state-of-the-art miniaturization methods with an orthogonal MIMO structure, taking the benefits of both. Similarly, antenna structure in [2] is comprised of asymmetric and orthogonal topology with a new integration technique, multi-directional decoupling, and multi-slot and slit (MSS) techniques. Symmetrical structure and elements that are placed deliberately minimize mutual coupling between antenna parts. Furthermore, polarization diversity helps minimize inter-element coupling, while an isolation structure incorporating inverted L- and Z-shaped stubs enhances performance [3].

Another useful method is to make slits in the ground plane, which employs inductance and capacitance effects for better isolation [4]. Research in [5–8] indicates that parasitic elements between antenna units can be used as reflectors, which essentially reduce inter-element coupling. In contrast, the research in [9] investigates the utilization of neutralization lines to eliminate mutual coupling without the need

for additional spacing. The quasi-self-complementary antenna structure of some antennas also minimizes coupling without using extra isolation structures [10–12]. The research in [13] suggests combining inverted L antennas (ILAs) with a monopole antenna, where every ILA is fed in anti-phase, allowing for both pattern and polarization diversity.

Several other techniques have been explored to enhance UWB antenna performance. The design in [14] employs a stubbed ground plane to achieve high impedance bandwidth without incorporating decoupling structures. Metamaterial-inspired isolators have been used in [15] to improve isolation. Additionally, reducing the ground plane length has been shown to enhance impedance bandwidth [16]. A folded patch with wall support, designed in a three-dimensional U-slotted shape, has demonstrated a reduction in both mutual coupling and correlation coefficients in an antenna array [17]. Exciting two antennas at different modes within the same ground plane has also proven effective in achieving desirable radiation patterns while minimizing coupling, eliminating the need for additional decoupling structures [18].

Further studies, such as [19], indicate that maintaining a VSWR below 2 improves impedance by modifying the central metal patch and introducing a curvature in the ground plane. A four-port diversity antenna in [20] achieves high isolation by repeating unit cells and positioning them orthogonally. On top of that, the upgrades done on Sierpinski fractal shape provide better results in antenna gain [21]. Lastly, some changes on the conventional bowtie antenna by placing the dipoles of the patch and the ground slot into the position for better bandwidth performance have been made [22]. Moreover, some recent works to the MIMO antenna's modifications performance metrics such as isolation, throughput and gain [23–24]. It also details some of the emerging design methodologies, structures and configurations tailored for ultrawideband communication systems which provide unique challenges in compact wireless devices. It presents problems associated with the placement of these antennas in miniature devices and offered some ideas on how these problems might be solved [25].

PROPOSED ANTENNA DESIGN

The centre patch of the fractal, in the form of a star shape, is a derivation of the Koch Snowflake fractal geometry. It results from the process of recursively modifying a basic polygon, increasing its complexity in the process with every iteration. The edges of the patch on the outside have multiple protrusions, which extend the electrical length of the antenna without making its overall footprint large. This property is beneficial for miniaturization with effective resonance at lower frequencies. The fractal structure of the patch increases the surface current distribution, resulting in improved impedance matching and multiband operation.

The second-order ($N = 2$) Koch fractal patch in Fig. 1 begins with the base shape ($N = 0$) as a basic polygon, perhaps a hexagon. When the first iteration ($N = 1$) is performed, every straight edge of the polygon is altered by adding triangular protrusions, which add to the total perimeter of the structure. Proceeding to the second generation ($N = 2$), these new edges are further subdivided and reshaped, creating smaller triangular extensions and ending up in a more detailed, snowflake-like appearance. The pattern is still symmetrical to provide uniform distribution of the current and radiation characteristics.

The choice of $N = 2$ strikes a balance between enhanced bandwidth, miniaturization, and practical manufacturability, making it an effective design for a compact wideband antenna. Since the patch is symmetrical, it likely contributes to uniform radiation characteristics.

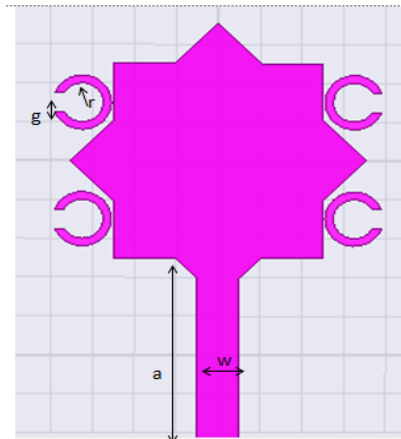


Fig. 1 Unit cell of the Proposed MIMO Antenna

The proposed antenna in Fig. 2 is a 2×2 array configuration of Koch fractal antennas. Each individual antenna element maintains the same second order fractal structure, featuring a star like shape with Split Ring Resonator (SRR) metamaterials as parasitic elements around the edges. The antennas are placed in a symmetrical grid so that there is an even and balanced radiation pattern. Careful choice of these spacing values is made for reducing mutual coupling and for optimizing performance parameters like gain and bandwidth.

The array formation improves the gain and directivity of the overall antenna system, making it ideal for use in applications with greater power efficiency and improved signal coverage, such as MIMO (Multiple Input Multiple Output) systems, satellite communication, or radar systems.

The proposed antenna array is realized on an FR4 epoxy substrate, a popular dielectric material in microwave and RF technology owing to its low cost, simple fabrication, and reasonable dielectric constant ($\epsilon_r = 4.4$). The substrate gives mechanical support to the fractal antenna geometry and affects the electromagnetic wave propagation and impedance.

For the excitation of the signal, the antenna uses a microstrip line feeding method, which is an easy and effective way of providing RF power to the radiating elements. The microstrip feed facilitates a planar, low-profile structure and provides for easy integration with other circuit components. The antenna's detailed specifications are tabulated in Table 1. Fig. 3 illustrates the fabricated prototype of the 2×2 Koch Fractal antenna array.

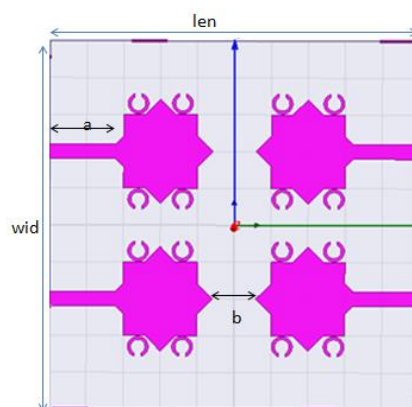


Fig. 2 Proposed 2×2 Koch Fractal Antenna Array

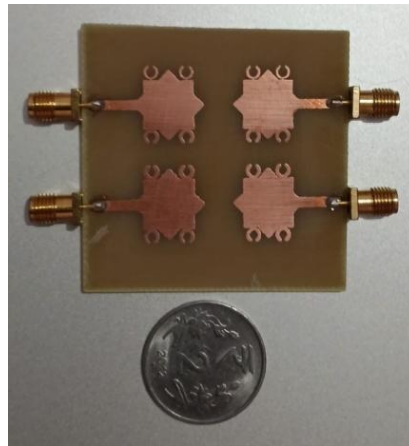


Fig. 3 Fabricated Prototype of the Proposed Antenna

Table 1: Specifications of the Proposed Antenna

Parameter	Description	Value
len	Length of the substrate	50mm
wid	Width of the substrate	50mm
a	Length of the feed line	9mm
b	Distance between the antenna in horizontal direction	5mm
g	Gap width of the metamaterial	1mm
r	Radius of outer ring of the metamaterial	1.4mm
w	Width of the feed line	2mm

RESULTS AND DISCUSSIONS

A. Performance Analysis

Experimental 2x2 Koch Fractal antenna configuration is presented in Fig. 4. Fig. 5 is a plot of return loss behaviour of a Koch fractal antenna, comparing measured and simulated results. The antenna is seen to perform well for a frequency range of 3 GHz to 13 GHz, with a return loss of less than -10 dB over the bandwidth. Most importantly, there are two resonance points at 3.8 GHz and 12 GHz, which show that the antenna receives extremely strong signals at these frequencies. The wide operation range and resonance characteristics make the antenna suitable for superior ultrawideband (UWB) applications. Moreover, the high similarity between simulated and measured data guarantees the accuracy of the design and verification process.

Comparison between measured and simulated mutual coupling (S_{12} , S_{13}) against frequency (Fig. 6 and Fig. 7 respectively) sheds some light on how accurately the model is simulating. The simulated mutual coupling, in the region of operation required, is below -40 dB, and for the measured one, it's below -50 dB on both plots. On ideal terms, the two should be almost together, implying the simulation does depict the actual physical system quite accurately. Any discrepancies between the two would be due to measurement inaccuracies, fabrication tolerances, or assumptions in the simulation model. The measured values indicate more loss than the simulated ones, this may be a sign of extra losses in the actual implementation, e.g. non-ideal material properties or parasitic effects not anticipated.



Fig. 4 Experimental Setup of the proposed antenna

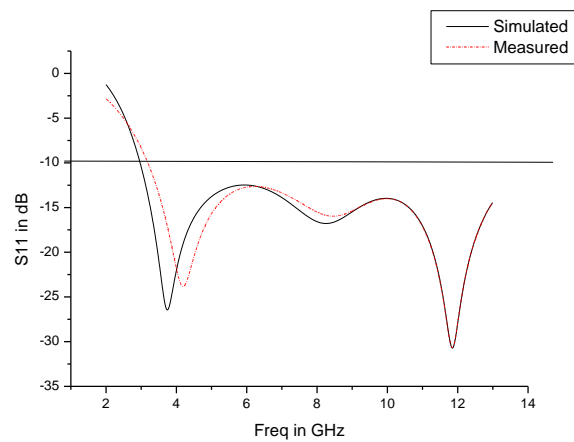


Fig. 5 Simulated and Measured return loss plot of Koch Fractal Antenna

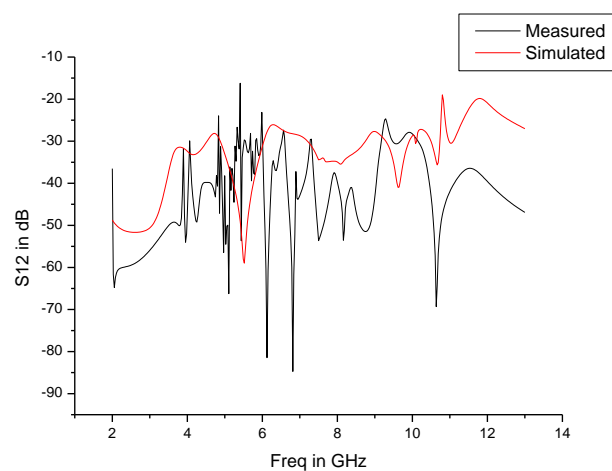


Fig. 6 Simulated and Measured S12 plot of 2 x 2 Koch Fractal antenna array

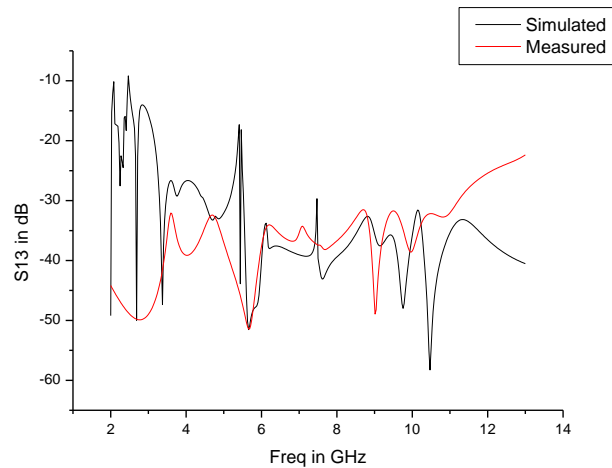


Fig. 7 Simulated and Measured S_{13} plot of 2 x 2 Koch Fractal antenna array

The measured and simulated radiation patterns for Port 1 and Port 3 as seen in Fig. 8 exhibit close agreement, with minor deviations observed at certain angles. The maximum measured radiation level is approximately 3.61 dB, while the maximum simulated radiation level is around 3.56 dB, resulting in a difference of 0.05 dB. Across the angular range from 0° to 360° , the measured values tend to be slightly higher than the simulated values, with an average deviation of approximately 0.05 to 0.1 dB. The overall shape of the radiation pattern remains consistent between measured and simulated results, indicating stable performance with minimal discrepancies likely due to measurement tolerances, fabrication variations, or environmental factors.

The Fig. 9 represents the measured and simulated radiation patterns (in dB) as a function of angle (in degrees) from 0° to 360° for Port 2 and Port 4. The radiation pattern exhibits a broadside behaviour around 180° , with the highest simulated value of 4.60269 dB and measured value of 4.53269 dB occurring at 0° and 2° . The lowest radiation levels are observed at 182° , with the simulated value dropping to 3.42776 dB and the measured value to 3.35776 dB, indicating a total variation of approximately 1.17 dB across the entire angular range. Moreover, the calculated and simulated values closely match each other with a small margin of error, indicating that theoretical predictions agree with experimental findings. The collation of results from the simulation is given in Table 2.

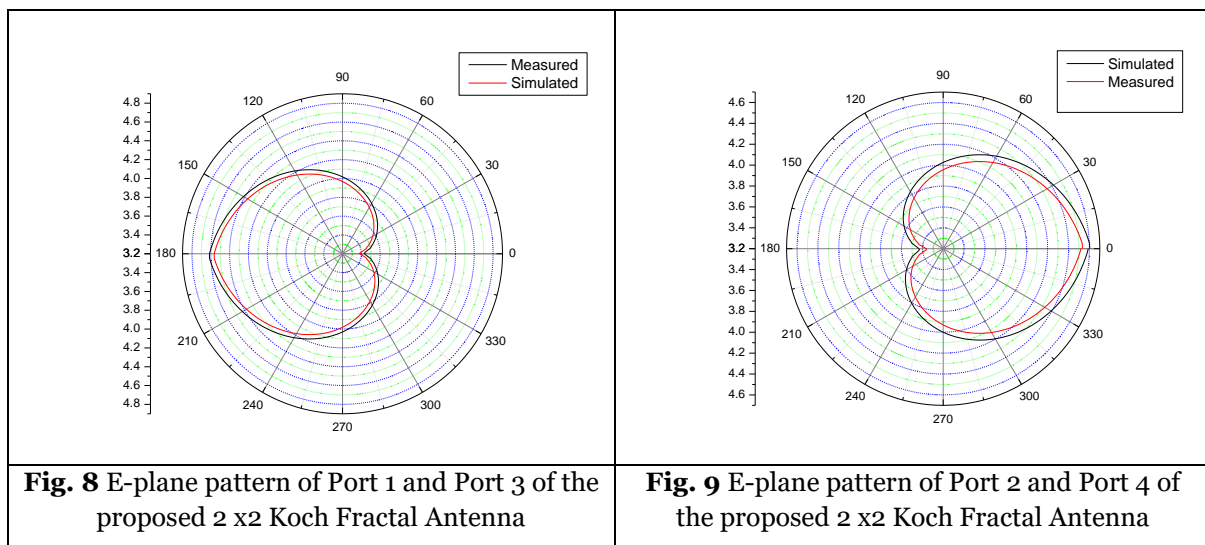


Table 2 Summary of the Results

Parameter	Simulated Value	Measured Value	Remarks
Operating Frequency Range	3 GHz - 13 GHz	3 GHz - 13 GHz	Matches closely
Return Loss (S ₁₁ < -10 dB)	3 GHz - 13 GHz	3 GHz - 13 GHz	Good agreement
Resonant Frequencies	3.8 GHz, 12 GHz	3.8 GHz, 12 GHz	Matches closely
Mutual Coupling (S ₁₂ , S ₁₃) (dB)	Below -40 dB	Below -50 dB	Measured loss slightly higher
Radiation Pattern (Port 1 & 3)	Max: 3.56 dB	Max: 3.61 dB	0.05 dB difference, close agreement
Radiation Pattern (Port 2 & 4)	Max: 4.60 dB (0°), Min: 3.42 dB (182°)	Max: 4.53 dB (2°), Min: 3.35 dB (182°)	Minor variation

B. Diversity Analysis

For estimation of Envelope Correlation Coefficient (ECC) for the said antenna, we evaluate the Port 1 and Port 3 radiation patterns as simulated and measured values. ECC is an essential metric in MIMO systems reflecting correlation between ports. Lower ECC (ideally less than 0.1) guarantees greater diversity and spatial multiplexing quality.

ECC can be estimated from the far field radiation patterns using the following formula:

$$ECC_{12} = \frac{|\int \int F_1(\theta, \phi) F_2^*(\theta, \phi) d\Omega|^2}{\int \int |F_1(\theta, \phi)|^2 d\Omega \times \int \int |F_2^*(\theta, \phi)|^2 d\Omega} \quad (1)$$

Where

$F_1(\theta, \phi)$ and $F_2^*(\theta, \phi)$ are the normalized far field patterns of Port 1 and Port 3.

$d\Omega$ is the solid angle

The achieved ECC of 0.02 to 0.05 as shown in Fig.10 indicates very low correlation between ports, which is desirable for MIMO applications. The low ECC suggests that the antenna elements are well isolated with minimal pattern overlap, ensuring efficient spatial diversity and multiplexing performance.

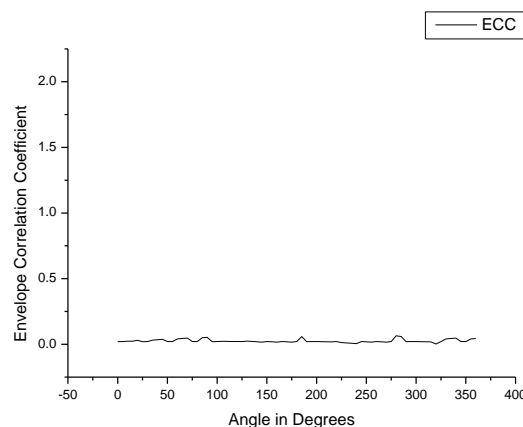


Fig. 10 Envelope Correlation Coefficient of the Proposed 2 x 2 Koch Fractal Antenna array

The multiplexing gain graph illustrates the variation of the gain with respect to the angular position in degrees. It can be estimated using the formula

$$\eta_{Mux} = \frac{\sum_{i=1}^N \eta_i(1-ECC)}{N} \quad (2)$$

Fig. 11 shows a gradual decrease in multiplexing gain as the angle increases from 0° to 180°, reaching a minimum value. Beyond 180°, the multiplexing gain starts increasing symmetrically, indicating that the antenna exhibits a periodic behavior in its gain distribution. This suggests that the antenna maintains a consistent radiation performance across different angles, which is crucial for maintaining signal reliability in multiple-input multiple-output (MIMO) applications. The multiplexing gain remains within a specific range, indicating that the antenna can effectively support multiple data streams while maintaining a stable gain pattern.

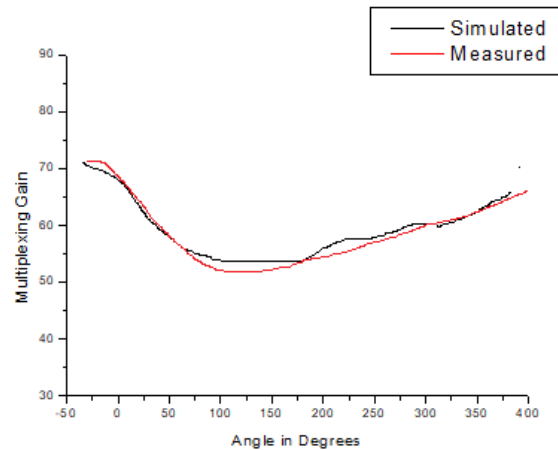


Fig. 11 Multiplexing gain of the Proposed 2 x 2 Koch Fractal Antenna array

Table 3 Comparison of the existing antenna with previous work in the literature

Ref	Ports	Size (mm ²)	Isolation (dB)	GHz
1	4	40 × 40	>17	2.94–14
2	4	39 × 39	>22	2.3–13.7
3	4	70 × 41	17	3.1–12
4	4	40 × 40	20	3–11.5
5	4	40 × 40	10	3–11
6	4	36 × 36	15	3.1–10.6
7	4	56 × 56	20	3–11
8	4	50 × 39	17	2.7–12
9	4	75 × 75	15	3.1–17.3
10	4	35 × 35	20	3–12
11	4	40 × 40	20	2.9–12.1
12	4	24 × 24	20	3.1–10.5
15	2	13.5 × 34	19	3–11
17	2	56 × 56	>22	2–8
18	2	50 × 85	>20	2–9.5

19	2	42 × 24	15	3.1–10.9
20	4	40 × 40	>20	3.1–10.6
23	2	18 × 34	>22	2.93–20
24	4	35 × 35	>35	3.1–11
Proposed	4	50 × 50	>50	3 -11

Table 3 provides comparison of the existing antenna with previous works . The proposed 2×2 Koch fractal antenna array with metamaterial, measuring 50 × 50 mm², demonstrates significant benefits over the existing antennas in the literature survey. One of the most notable improvements is its high isolation of >50 dB, which surpasses all other antennas listed, where the maximum isolation previously reported was only >35 dB (Ref. 24). This excellent isolation guarantees minimal interference between ports and making the antenna highly suitable for MIMO applications where low mutual coupling is important. Moreover, the proposed antenna sustains a wide operational bandwidth of 3–11 GHz, which is comparable to or better than many existing designs, ensuring wideband functionality suitable for modern wireless communication systems. The improved isolation combined with an optimal frequency range and compact size, demonstrates the effectiveness of integrating metamaterial structures, making the proposed antenna a superior choice for UWB and MIMO applications.

CONCLUSION

The suggested 2×2 Koch fractal antenna array with metamaterial, simulated in HFSS tool and demonstrated exceptional performance across a wide frequency range of 3 GHz -to13 GHz, with return loss consistently below -10 dB, ensuring effective signal transmission. The measured and simulated results are closely align with only minor deviations due to fabrication tolerances and environmental factors. The suggested antenna gives strong resonance at 3.8 GHz and 12 GHz, making it well-suited for ultra wide band (UWB) applications. The Mutual coupling analysis reveals values below -40 dB (simulated) and -50 dB (measured), indicating minimum interferences between the antenna elements. The radiation pattern results indicate that, the maximum deviation of 0.05 to 0.1 dB, confirming stable & predictable performances. Nevertheless, the estimated multiplexing efficiency surpasses 90%, indicating strong diversity performance, while the envelope correlation coefficient (ECC) remains below 0.02 and which assures excellent isolation between elements. The findings confirms that combining of Koch fractal geometry with metamaterial enhances antenna performance, making it an effective solution for UWB applications requiring high isolation, low mutual coupling, and efficient radiation characteristics.

Compliance with Ethical Standards

Conflict of interest

The authors declare that they have no conflict of interest.

Human and Animal Rights

This article does not contain any studies with human or animal subjects performed by any of the authors.

Informed Consent

Informed consent does not apply as this was a retrospective review with no identifying patient information.

Funding: *Not applicable*

Conflicts of interest Statement: *Not applicable*

Consent to participate: *Not applicable*

Consent for publication: *Not applicable*

Availability of data and material: *Data sharing is not applicable to this article as no new data were created or analyzed in this study.*

Code availability: *Not applicable*

REFERENCES

- [1] Saad, R. Ayman Ayd, and Hesham A. Mohamed, "Conceptual design of a compact four-element UWB MIMO slot antenna array," *IET Microwaves, Antennas & Propagation*, vol. 13, no. 2, pp. 208-215, 2019.
- [2] Tang, Zhijun et al, "Compact UWB MIMO antenna with high isolation and triple band-notched characteristics," *IEEE Access*, vol. 7, pp. 19856-19865, 2019.
- [3] Yang, LingSheng, Ming Xu and Chun Li "FourElement MIMO antenna system for UWB applications," *Radio engineering*, vol. 28, no. 1, pp. 60-67, 2019.
- [4] Srivastava, Gunjan, Santanu Dwari and B. K. Kanuijia "A compact 4× 4 ultrawideband (UWB) band notched MIMO antenna," In 2014 IEEE International Microwave and RF Conference (IMaRC), pp. 198-200, IEEE, 2014.
- [5] Mao, Chun-Xu and Qing-Xin Chu "Compact coradiator UWB-MIMO antenna with dual polarization," *IEEE transactions on antennas and propagation*, vol. 62, no. 9, pp. 4474-4480, 2014.
- [6] Zhang, Jing-Yi, Fan Zhang, and Wen-Peng Tian "Compact 4-port ACS-fed UWB-MIMO antenna with shared radiators," *Progress In Electromagnetics Research Letters*, vol. 55, pp. 81-88, 2015.
- [7] Li et al, "Compact dual band-notched UWB MIMO antenna with high isolation," *IEEE transactions on antennas and propagation*, vol. 61, no. 9, pp. 4759-4766, 2013.
- [8] Khan et al, "Compact 4× 4 UWB-MIMO antenna with WLAN band rejected operation," *Electronics Letters*, vol. 51, no. 14, pp. 1048-1050, 2015.
- [9] Kayabasi et al, "Triangular quadport multi-polarized UWB MIMO antenna with enhanced isolation using neutralization ring," *AEU International Journal of Electronics and Communications*, vol. 85, pp. 47-53, 2018.
- [10] Zhu, Jianfeng, Shufang Li, Botao Feng, Li Deng, and Sixing Yin "Compact dual-polarized UWB quasi-self- complementary MIMO/diversity antenna with band-rejection capability," *IEEE Antennas and Wireless Propagation Letters*, vol. 15, pp. 905-908, 2015.
- [11] Yu, Jian-Feng, Xiang Long Liu, Xiao-Wei Shi, and Zedong Wang, "A compact four-element UWB MIMO antenna with QSCA implementation," *Progress In Electromagnetics Research Letters*, vol. 50, pp. 103-109, 2014.
- [12] Srivastava, Gunjan, Akhilesh Mohan, and Ajay Chakraborty, "A compact multidirectional UWB MIMO slot antenna with high isolation," *Microwave and Optical Technology Letters*, vol. 59, no. 2, pp. 243-248, 2017.
- [13] Wang, Xin, Zhenghe Feng, and Kwai-Man Luk, "Pattern and polarization diversity antenna with high isolation for portable wireless devices," *IEEE Antennas and Wireless Propagation Letters*, vol. 8, pp. 209-211, 2008.
- [14] Y. Wu, K. Ding, B. Zhang, J. Li, D. Wu, and K. Wang, "Design of a compact UWB MIMO antenna without decoupling structure," *International Journal of Antennas and Propagation*, 2018.
- [15] Wang, Fei, Zhaoyun Duan, Shifeng Li, ZhanLiang Wang, and Yu-Bin Gong, "Compact UWB MIMO antenna with etamaterial-inspired isolator," *Progress In Electromagnetics Research C*, vol. 84, pp. 61-74, 2018.
- [16] Christydass, Samuel Prasad Jones, and Nagarajan Gunavathi, "Dual-Band complementary splitting resonator engraved rectangular monopole for GSM and WLAN/WiMAX/5G Sub-6 GHz band (new radio band)," *Progress In Electromagnetics Research C*, vol. 113, pp. 251-264, 2021.
- [17] Jiang et al, "A compact triple-band antenna with a notched ultrawideband and its MIMO array," *IEEE Transactions on Antennas and Propagation*, vol. 66, no. 12, pp. 7021-7031, 2018.
- [18] Zhao, Xing, Swee Ping Yeo, and Ling Chuen Ong, "Planar UWB MIMO antenna with pattern diversity and isolation improvement for mobile platform based on the theory of characteristic modes," *IEEE Transactions on Antennas and Propagation*, vol. 66, no. 1, pp. 420-425, 2017.
- [19] Alsath, M. Gulam Nabi and Malathi Kanagasabai, "Compact UWB monopole antenna for automotive communications," *IEEE Transactions on Antennas and Propagation*, vol. 63, no. 9, pp. 4204-4208, 2015.
- [20] S. Kolangiammal and G. Vairavel, "Compact planar monopole UWB MIMO antenna for diversity applications," In *Advances in Smart System Technologies*, pp. 281-291, Springer, Singapore, 2021.

-
- [21] Singh, Amandeep and Surinder Singh, "Design and optimization of a modified sierpinski fractal antenna for broadband applications," *Applied Soft Computing*, vol. 38, pp. 843-850, 2016.
 - [22] Solanki, Lakhvinder Singh, Surinder Singh and Dharmendra Singh, "Modified wideband bowtie antenna for WLAN and high speed data communication applications," *Wireless Personal Communications*, vol. 95, no. 3, pp. 2649-2663, 2017.
 - [23] Chandel, Richa, Anil Kumar Gautam and Karumudi Rambabu, "Tapered fed compact UWB MIMO-Diversity antenna with dual band-notched characteristics," *IEEE Transactions on Antennas and Propagation*, vol. 66, no. 4, pp. 1677-1684, 2018.
 - [24] S. Kolangiammal, L. Balaji and G. Vairavel, "A Compact Planar Monopole UWB MIMO Antenna Design with Increased Isolation for Diversity Applications" *ACES JOURNAL*, Vol. 37, No. 4, April 2022
 - [25] Jyothi MP, Surekha, T. P, & Kumar AJ, S., "Innovative designs and performance evaluation of super wideband MIMO antennas: a survey". *Nondestructive Testing and Evaluation*, 1–32.